D^* production by real and virtual photons at HERA

Ralf Gerhards
Deutsches Elektronen Synchrotron, Notkestraße 85, D - 22603 Hamburg
representing the H1 Collaboration

Recent results from the H1 experiment are presented for open charm production in *ep* collisions at HERA. Cross sections for $D^{*\pm}$ production at $Q^2 < 100$ GeV^2 (Deep Inelastic Scattering) and in the photoproduction limit $Q^2 \to 0$ are discussed and a direct extraction of the gluon distribution in the proton in the framework of NLO QCD is presented. The measurements are compared to NLO QCD calculations.

At HERA, positrons of 27.5 GeV collide with 820 GeV protons yielding a center-of-mass (cm) energy of 300 GeV.

Heavy flavours are predominantly produced in pairs by the photon gluon fusion process. The cross section is large and allows to test the description of the production process by perturbative QCD and to extract information on the parton distributions of the initial state proton (and photon).

The scattering cross section is dominated by processes in which the momentum transfer Q^2 in the scattering process is small ($Q^2 \approx 0$; photoproduction). Data in the deep inelastic rsattering (DIS) regime correspond to large γ virtualities ($Q^2 > 1\,\mathrm{GeV}^2$). The $\gamma^{(*)}p$ cm energies are as high as $W_{\gamma p} \approx 100 \div 200\,GeV$ and thus the HERA experiments extend the reach of fixed target experiments by about one order of magnitude.

The present discussion will focus on analyses of D^{*+} production in photoproduction and DIS [1], using data taken with the H1 experiment [2] during the years 1994 to 1996, corresponding to a luminosity of about 10 pb^{-1}.

Open charm has been reconstructed in the fragmentation and decay chain $c \to D^{*+} \to D^0\pi^+ \to (K^-\pi^+)\pi^+$ (and its charge conjugate).

The total open charm photoproduction cross section has been measured at HERA [3] at cm energies $W_{\gamma p}$ up to 230 GeV and is found to be an order of magnitude larger than at fixed target energies (Fig. 1). Good agreement is observed with QCD calculations in next-to-leading order (NLO) [4]. The data starts to provide some lever arm

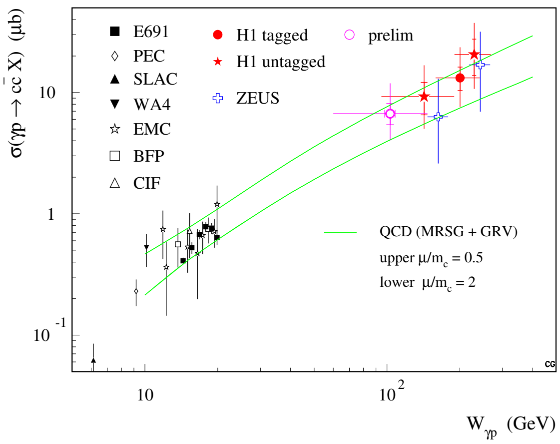

Figure 1. Total photoproduction cross section $\sigma(\gamma p) \to c\bar{c}X$ as function of $W_{\gamma p}$.

on the slope of the cross section versus energy, which is related to the x dependence of the gluon density on the proton. However, there are large uncertainties in the extrapolation from the visible to the total cross section involved which depend on the parton densities in the proton and in the photon and on the charm quark mass. Thus it is nor straightforward to interprete the total cross section in these terms.

The NLO QCD calculations are performed in the massive scheme [4,5] in which charm quarks are treated as massive particles, only generated perturbatively in the final state, whereas the three light flavours and gluons are the active partons in the initial state proton and photon. This scheme is valid as long as the transverse momentum, p_T of the charm quark is not too large with respect to its mass. It is indispensible for the calculation of the total cross section. If $p_T \gg m_c$, the massless scheme [6] with charm an active flavour in the proton, should work particularly well.

The calculations are fully differential and thus allow to predict cross sections differential in any final state variable and in the kinematical range of the analysis. Non-pertubative fragmentation effects are taken into account by supplementing the exact NLO calculation with fragmentation models [7].

Differential cross sections as function of rapidity and transverse momentum have been measured both in photoproduction and DIS. The DIS measurement is shown in Fig. 2 in comparison with the prediction of the NLO QCD calculation [5], which shows reasonable agreement, except for

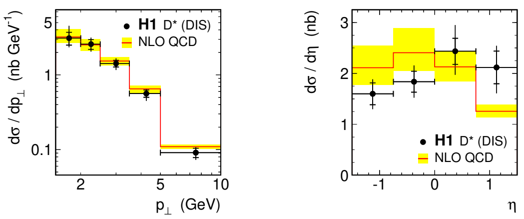

Figure 2. Differential cross sections for $ep \rightarrow eD^{*+}X$ in the kinematical range of experimental acceptance.

the rapidity distribution where the data tends to lie below (above) the theoretical expection for negative (positive) pseudorapidities, corresponding to the directions of the incoming positron (proton). The description can be improved by adjusting the parameters of the calculation within reasonable values.

In photoproduction, double differential cross sections in terms of transverse momentum and rapidity ($\hat{y}$) have been measured (Fig. 3). The data is dominated by $p_T \approx m_c$ so that the calculation in the massive scheme (histogram) is expected to provide a good description of the process in this regime, which is indeed observed. The

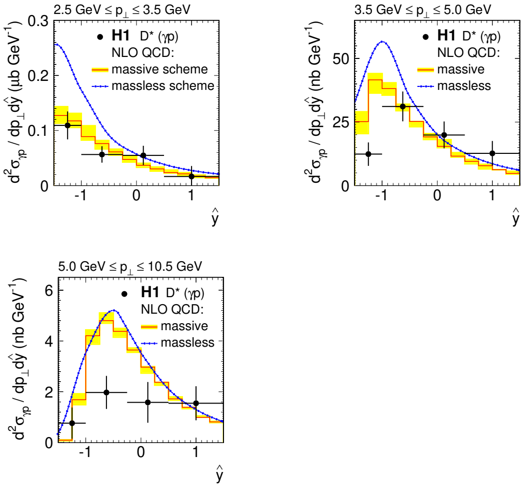

Figure 3. Double differential cross sections for $\gamma p \rightarrow c\bar{c}X$ for three different ranges of transverse momentum at an average $W_{\gamma p}$.

massless calculation (solid line) as expected fails to describe the data in the region $p_T \approx m_c$. Both models fail to describe the measured rapidity distribution in the upper p_T range. It has been verified that the observed deviations in the tails have no impact on the extraction of the gluon density distribution of the proton described below.

Having verified that the NLO calculations give a reasonable description of the data, the gluon distribution of the proton is extracted both from the photoproduction and DIS data. The observed momentum fraction of the gluon, x_g^{obs}, is reconstructed from the kinematics of the final state and a differential cross section $d\sigma/dx_g^{obs}$ is determined, which for the DIS data is shown in Fig. 4. The correlation of x_g^{obs} with the true x_g as given by the NLO QCD calculations is used in an iterative unfolding procedure [8] to obtain x_g. The gluon density is then obtained by reweighting the calculation with the measured cross section. The resulting distribution $x_g g(x_g)$ is shown in Fig. 5 together with the CTEQ4F3 parametrization [9]. The range $10^{-3} < x_g < 0.02$ is covered, which — due to the smaller invariant mass of the final state partons in reach — extends the previous H1 measurement of the momentum distribution

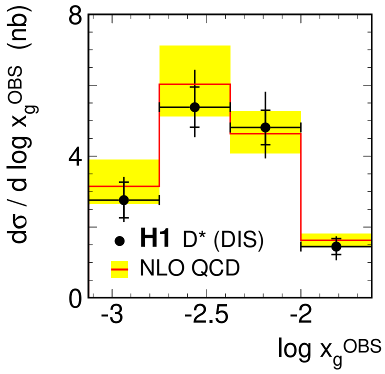

Figure 4. Differential cross section for $ep \to eD^*X$ as function of x_g^{obs} in the visible range compared to NLO QCD prediction.

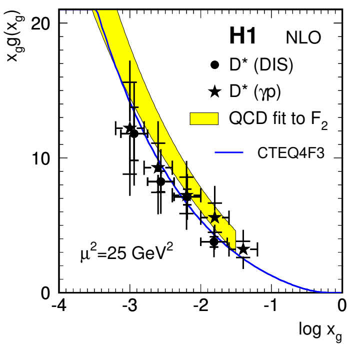

Figure 5. Gluon densities obtained from the D^* analyses in photoproduction and DIS. For comparison the H1 QCD analysis of the inclusive F_2 measurement (dashed band) and the CTEQ4F3 parametrization are shown.

from di-jet events [10] to smaller x_g. The systematic error is dominated by the uncertainties of the charm quark mass and the scale. The data from photoproduction and DIS agree well within the large errors. They also agree with the result from an analysis of scaling violations in the inclusive measurement of F_2 [11].

In conclusion, measurements of total and differential $D^{*\pm}$ production cross sections in ep collisions at HERA have been presented. Reasonable agreement is found with NLO perturbative QCD calculations in the region of experimental acceptance.

The gluon distribution of the proton has been been extracted both in the photoproduction and deep inelastic scattering regimes. The measurements show good agreement with each other and also with the (indirect) determination from scaling violations of F_2, demonstrating the universality of the gluon distribution in the proton within the framework of NLO QCD.

Acknowledgements: I would like to thank Max Klein and his team for perfect organization of a stimulating workshop at such a nice place as Zeuthen. I am grateful to my colleagues of the H1 Collaboration for providing the beautiful analyses and many interesting discussions.

REFERENCES

1. C. Adloff et al. (H1 Coll.), Nucl. Phys. **B545** (1999) 21.
2. I. Abt et al. (H1 Coll.), Nucl. Instr. Meth. **A386** (1997) 310 and 348.
3. M.Derrick et al. (ZEUS Coll.), Phys. Lett. **B349** (1995) 225; S. Aid et al. (H1 Coll.), Nucl. Phys. **B472** (1996) 32.
4. S. Frixione et al., Phys. Lett. **B348** (1995) 633; Nucl.Phys. **B454** (1995) 3.
5. B.W. Harris and J. Smith, Phys. Rev. **D57** (1998) 2806.
6. B.A. Kniehl, G. Kramer and M. Spira, Z. Phys. **C76** (1997) 689; M. Cacciari, M. Greco, Phys. Rev. **D55** (1997) 7134; J. Binnewies, B.A. Kniehl and G.Kramer, Z. Phys. **C76** (1997) 677.
7. C. Peterson et al., Phys. Rev. **D27** (1983) 105.
8. G. D'Agostini, Nucl. Instr. Meth. **A362** (1995) 487.
9. H. Lai et al., Phys. Rev. **D55** (1997) 1280.
10. S. Aid et al. (H1 Coll.), Nucl. Phys. **B449** (1995) 3.
11. S. Aid et al. (H1 Coll.), Nucl. Phys. **B470** (1996) 3.